https://doi.org/10.48048/tis.2022.5777

Temperature-Related Electronic Low-Lying States in Different Shapes $In_{.1}Ga_{.9}N/GaN$ Double Quantum Wells under Size Effects

Walid Belaid[1,2], Haddou El Ghazi[1,3,*], Redouane En-Nadir[1], Hamdi Şükür Kılıç[2,4,5], Izeddine Zorkani[1] and Anouar Jorio[1]

[1]Solid State Physics Laboratory (SSPL), Department of Physics, Faculty of Science, Mohammed Ben Abdellah University, Fes, Morocco
[2]Laser Spectroscopy Group (LSG), Department of Physics, Faculty of Science, University of Selcuk, Campus, Selcuklu, Konya, Turkey
[3]MPSI Group, ENSAM Laboratory, ENSAM, Hassan II University, Casablanca, Morocco
[4]University of Selçuk, Directorate of Laser Induced Proton Therapy Application and Research Center (Manager), Selçuklu, Konya, Turkey
[5]University of Selçuk, Directorate of High Technology Research and Application Center, Selçuklu, Konya, Turkey

([*]Corresponding author's e-mail: hadghazi@gmail.com)

Received: 5 June 2021, Revised: 27 July 2021, Accepted: 31 July 2021

Abstract

In this paper, we report the electronic states of hydrogenic impurity in InGaN/GaN double quantum wells (DQWs) with different shapes using a numerical procedure within the effective mass approximation. The effects of temperature, impurity position and size on the 1S-, 2S- and 2P-low-lying states are investigated for rectangular, parabolic and triangular finite potential confinements. Our results reveal that the binding energy versus the well width displays a maximum value around the effective Bohr radius and a larger value is obtained for rectangular compared to parabolic and triangular profiles. Moreover, regardless the size and impurity's position, it is found that the main impact of the temperature is to shrink the binding energy. It is obtained that the binding energy drop is about 3.48 meV for rectangular and 4.26 meV for both parabolic and triangular profiles. Moreover, as the impurity is moved from the right barrier center to the structure center, the 1S-binding energy improvement is about 77.6 % in rectangular whereas it exceeds 91.4 % for other profiles. It is established that the binding energy can be easily modulated by adjusting the temperature, structure size and impurity's position. The results we obtained agree quite well with the findings.

Keywords: Binding energy, Double quantum wells, Coupling, (In,Ga)N, Temperature

Introduction

Group-III nitrides inherent properties, such as its direct band-gap, adjustable from 0.64 to 3.38 eV [1], [2], radiation resistance [5] and high absorption coefficient [3,4], and also make the ternary (In,Ga)N compound semiconductor material an tremendous attractive candidate for photovoltaic applications, light-emitting diodes (LEDs) and Laser diodes [6]. Due to the importance of low-dimensional Nano-systems in the development of new semiconductor devices and applications, the effects of external perturbation such as electric field, magnetic field, temperature and pressure on their physical and chemical properties constitute a subject of considerable interest from both theoretical and technological point of view. Through several papers in the literature [7-28], the temperature effect modifying the energy levels, the masses of carriers; the dielectric constant, the potential barrier, the stability of exciton and the Γ–X band cross over on the ground-state as well as of some low-lying excited states is reported. This effect has been investigated by Elabsy [9] and Nithiananthi and Jayakumar [10] in a $GaAs/Ga_{1-x}Al_xAs$ quantum well, and Khordad [11] in a V-groove $GaAs/Ga_{1-x}Al_xAs$ quantum wire. Recently, the electronic properties were examined using different methods: Variational approach [12-15], finite element method [16,17], finite difference method [18], matrix

diagonalization method [19] and density functional theory [20]. However, few papers have dealt with the electronic properties of multiple low-dimensional systems in the presence of a hydrogenic donor impurity [21-24]. Multiple quantum wells (MQWs) based on InGaN/GaN structures with high structural and optical qualities have also been successfully fabricated and extensively investigated [25]. In addition, based on symmetric and asymmetric multiple quantum wells (MQWs) systems, several theoretical papers are reported in the literature such as double inverse parabolic quantum wells (DIPQW) [26], double symmetric and asymmetric quantum wells [27,28].

In this paper, we were focused on the effects of the temperature, impurity position, coupling (Middle) and side barrier widths on the binding energy of ground state and low-lying excited states in the presence of a hydrogenic impurity in (In,Ga)N/GaN rectangular (DRQW), parabolic (DPQW) and triangular (DTQW) double quantum wells. This work is organized as follows: We briefly describe the theoretical model in section 2 while the numerical results are presented and discussed in section 3. Finally, the conclusion is given in section 4.

Theoretical framework

In the present work we deal with an on-center hydrogenic shallow-donor impurity in WZ (In,Ga)N/GaN rectangular (DRQW), parabolic (DPQW) and triangular (DTQW) double quantum wells of a height $V_0(x,T)$, side barriers width (L), coupling barrier width (H) and a well width (l). The description of the nanostructures under study is included in **Figure 1** and the corresponding confinement potential shapes are given in Eqs. (2) - (4).

Within the framework of single-band effective-mass and the parabolic band approximations, the electron Hamiltonian in the presence of a shallow-donor impurity in the $In_xGa_{1-x}N$ nanostructures can be written as:

$$H = -\frac{\hbar^2}{2}\vec{\nabla}\left(\frac{1}{m^*(x,,z,T)}\vec{\nabla}\right) - \frac{e^2}{\varepsilon_0\varepsilon^*(x,z,T)|\vec{r}-\vec{r}_0|} + V(z) \quad (1)$$

e is the electron charge, $\hbar$ is the reduced Planck constant, x measures the Indium fraction in the ternary, ε_0 is the vacuum permittivity, z is the growth direction coordinate, $|\vec{r} - \vec{r}_0|$ is the electron-impurity distance and $V\ (z)$ is the finite potential barrier given for each profile as:

Double rectangular quantum wells

$$\mathrm{V_r(z)} = \begin{cases} 0 & \mathrm{L} < z < L + l \ \ and \\ & \mathrm{L} + H + l < z < L + H + 2l \\ V_0(\mathrm{x,T}) & \text{elsewhere} \end{cases} \quad (2)$$

Double parabolic quantum wells

$$\mathrm{V_p(z)} = \begin{cases} \left(\frac{4}{l^2}\right)\left(z - L - \frac{l}{2}\right)^2 V_0(\mathrm{x,T}) & \mathrm{L} < z < L + l \\ \left(\frac{4}{l^2}\right)\left(z - L - H - 3\frac{l}{2}\right)^2 V_0(\mathrm{x,T}) & \mathrm{L} + H + l < z < L + H + 2l \\ V_0(\mathrm{x,T}) & \text{elsewhere} \end{cases} \quad (3)$$

Double triangular quantum wells

$$V_t(z) = \begin{cases} \left(-\frac{2}{l}\right)\left(z - L - \frac{l}{2}\right)V_0(x,T) & L < z < L + \frac{l}{2} \\ \left(\frac{2}{l}\right)\left(z - L - \frac{l}{2}\right)V_0(x,T) & L + \frac{l}{2} < z < L + l \\ \left(-\frac{2}{l}\right)\left(z - L - H - 3\frac{l}{2}\right)V_0(x,T) & L + H + l < z < L + H + 3\frac{l}{2} \\ \left(\frac{2}{l}\right)\left(z - L - H - 3\frac{l}{2}\right)V_0(x,T) & L + H + 3\frac{l}{2} < z < L + H + 2l \\ V_0(x,T) & \text{elsewhere} \end{cases} \quad (4)$$

$V_0(x,T) = Q.\Delta Eg(x,T)$ is the height of the potential barrier while ($Q = 0.7$) and $\Delta Eg(x,T)$ are, respectively the conduction band off-set parameter and the difference between the band gap energies of GaN and $In_xGa_{1-x}N$ semiconductor materials.

According to [29], the temperature-dependent band-gap energy is given as following:

$$E_g(T) = E_g(0) - \frac{\alpha.T^2}{T+\beta} \quad (5)$$

For $In_xGa_{1-x}N$, the band-gap energy is obtained as the interpolation between InN and GaN corrected by the bowing parameter ($b = 1.40$) [30]:

$$E_g^{In_xGa_{1-x}N}(x,T) = x.E_g^{InN}(T) + (1-x).E_g^{GaN}(T) - b.(1-x).x \quad (6)$$

where, $E_g^{InN}$and $E_g^{GaN}$are respectively the band-gap energies of InN and GaN, while b is the band-gap bowing parameter taking into account of band-gap non-linearity dependence as a function of the indium composition. In this paper, the parameters reported by Vurgaftam and Meyer [7] listed in **Table 1** are used in our calculation.

Table 1 The parameters used in the computation [7].

	E_g (0 K) (eV)	α ($meV \cdot K^{-1}$)	β (K)	ε^*(300 K) (ε_0)	C (eV)
GaN	3.299	0.909	830	9.8	14.07
InN	0.78	0.245	624	13.7	25.50

The indium composition dependence of $In_xGa_{1-x}N$ electron mass is calculated by linear interpolation between GaN and InN. It is given as:

$$m^*(x,z,T) = \begin{cases} x.m^*_{InN}(T) + (1-x).m^*_{GaN}(T) & in\ the\ wells \\ m^*_{GaN}(T) & in\ the\ barriers \end{cases} \quad (7)$$

$m^*(T)$ is the temperature-dependent effective-mass. According to $\vec{k}\cdot\vec{P}$ theory, the temperature-dependent effective-mass is given by the formulas [30]:

$$\frac{m_0}{m^*(T)} = 1 + \frac{C}{E_g(T)} \quad (8)$$

$E_g(T)$ is the band-gap temperature dependency, m_0 is the free electron mass while C is the energy related to the momentum matrix element, and it is a constant for each material.

The relative dielectric constants $\varepsilon^*(x,z,T)$ for GaN and $In_xGa_{1-x}N$ versus the temperature are given by [31].

$$\varepsilon^*(x,z,T) = \varepsilon^*_{GaN}(300K).exp\left[\frac{T-300}{10^4}\right] \qquad in\ the\ barriers \tag{9}$$

$$\varepsilon^*(x,z,T) = \varepsilon^*_{GaN}(T) + 6{,}4.x \qquad in\ the\ wells \tag{10}$$

At the interface between the well and the barrier, there is an overlap between GaN and $InGaN$ materials. Thus, as we adopted in our recent work [32], the relative dielectric constant at the interfaces is expressed as follows:

$$\varepsilon^*_{Interfaces} = \sqrt{\varepsilon^*_{GaN}.\varepsilon^*_{InGaN}} \tag{11}$$

The binding energy known as the difference between the eigen-state without and with impurity is computed for 1S, 2S- and 2P-states.

For such a problem, the analytical Schrödinger equation solving is impossible and subsequently, the finite difference method is adopted to obtain the eigen-values and their corresponding eigen-functions of the Hamiltonian given in Eq. (12). For this reason, a mono-directional mesh (calculation grid) composed of $5N+1$ points is considered. We have characterized each layer (Well, barrier) by a different discretization step. We have assigned $h_w\left(=\frac{l}{N}\right)$, $h_I\left(=\frac{H}{N}\right)$ and $h_b\left(=\frac{L}{N}\right)$ for the well, coupling barrier and side-barriers, respectively. So, the mesh's nodes of all layers are expressed, respectively as $z_j = jh_b$, $z_j = L + jh_w$, $z_j = L + l + jh_I$, $z_j = L + l + H + jh_w$ and $z_j = L + H + 2l + jh_b$ for $0 \le \mathrm{j} \le N$.

The first and second derivatives of the particle wave-function are given as following:

$$\begin{cases} \left(\frac{d^2\Psi_i(z)}{dz^2}\right)_{z=z_j} = \frac{\Psi_i^{j+1} - 2\,\Psi_i^j + \Psi_i^{j-1}}{h^2} \\ \left(\frac{d\Psi_i(z)}{dz}\right)_{z=z_j} = \frac{\Psi_i^{j+1} - \Psi_i^j}{h} \end{cases} \tag{12}$$

Numerical results and discussion

In this section, we present numerical results for the temperature, size, impurity position and coupling effects on the ground, first and second excited states in finite InGaN/GaN rectangular (DRQW), parabolic (DPQW) and triangular (DTQW) double quantum wells. The results are given in the effective units, i.e., the effective Bohr radius $a_b^* = \frac{\varepsilon_0\hbar^2}{m^*e^2}$ as the unit of length.

In order to facilitate the interpretation of the binding energy results, we have presented primarily the probability densities of all states in **Figure 1**.The main common characteristic is the fact that the electronic wave-functions are symmetrically distributed. In addition, the ground and first excited states are mainly located in the wells (InGaN regions) while the second excited one is principally located in the barrier (GaN) especially for rectangular-shape. However, for parabolic and triangular shapes, the states are located in the barriers due to the strong confinement compared to rectangular profile.

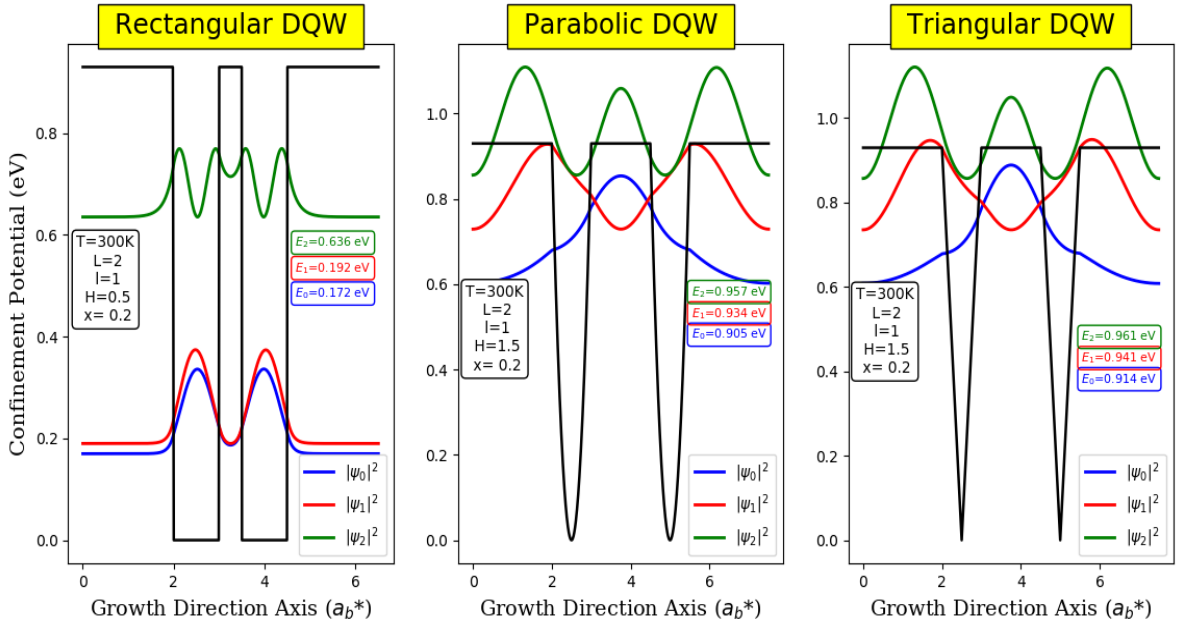

Figure 1 Probability density of 1s, 2s and 2p states in finite InGaN/GaNon-center donor impurity DRQW, DPQW and DTQW as a function of the growth direction. The potential profile shapes are included.

In **Figure 2**, we present our computed results for the ground, first and second excited states energies in the presence (a) absence (b) of the impurity for different $In_{.1}Ga_{.9}N/GaN$ DQW-shapes versus the well width. These results are obtained for $T = 0, 300$ and $900\ K$ and ($L = 1,\ H = 1.5$). As illustrated by these figures, for a fixed temperature the electron-energy monotonically decreases according to the well width as expected. The curves show similar behavior for all structures for both cases with and without impurity. It is clearly seen that the presence of the impurity leads to the drop of the electron energy which can be due to the Coulomb interaction. It is obviously shown that the electron energy decreases when the temperature increases for all the well widths. This can be assigned to the effective-mass, dielectric constant and potential barrier height dependence according to the temperature as reported in **Table 2**. It is important to mention that this behavior is quite significant in parabolic and triangular DQWs compared to rectangular one.

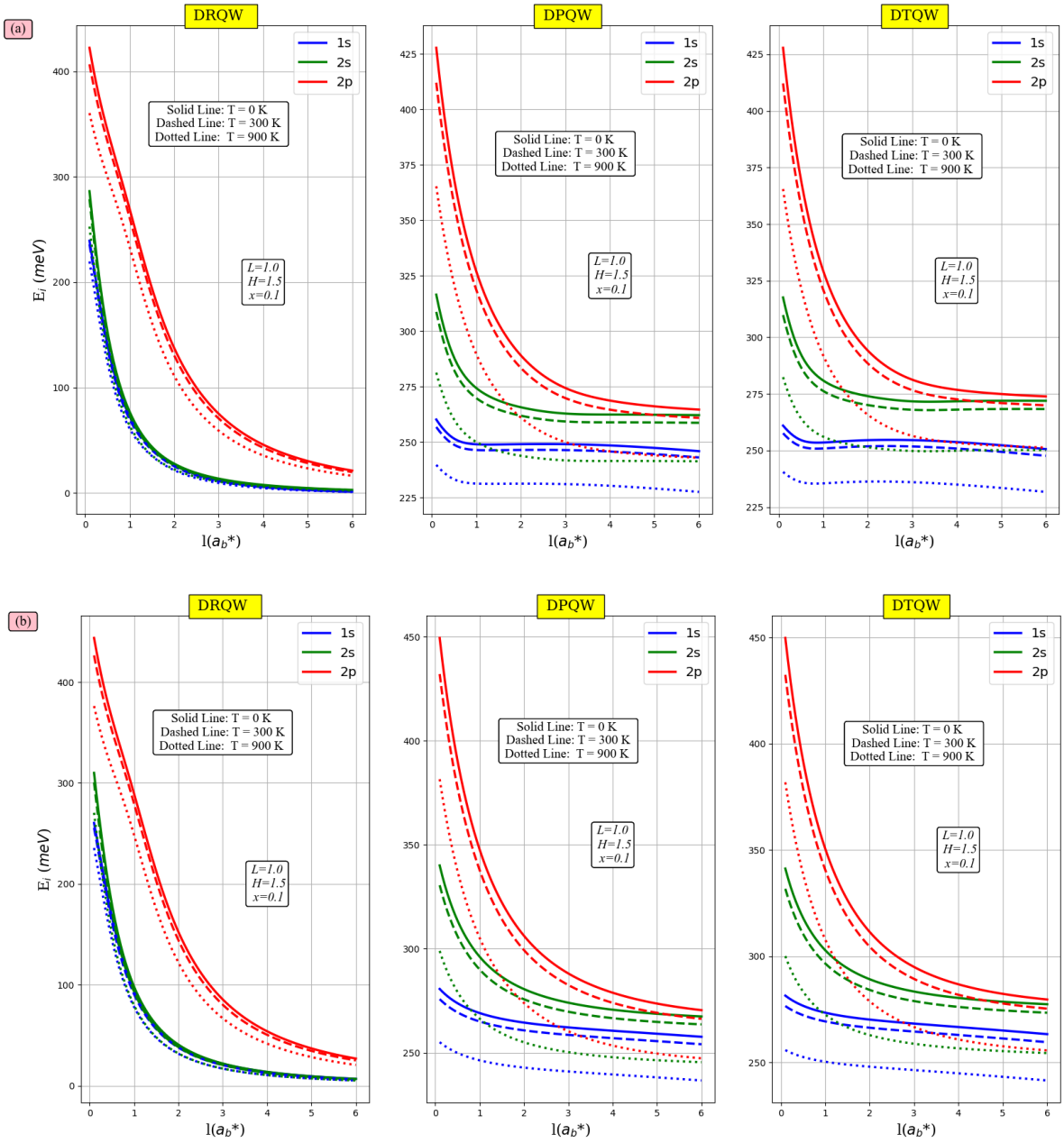

Figure 2 Variation of the donor 1S, 2S and 2P-states energies versus the well width in a $GaN/In_{0.25}Ga_{0.75}N$ rectangular, parabolic and triangular DQWs for fixed parameters $L = 1$ and $H = 1.5$ in the presence (a) absence (b) of the impurity at $T = 0\,K$ (solid curve), $T = 300\,K$ (dashed curve) and $T = 900\,K$ (dotted curve).

Table 2 The variation of the barrier height, effective mass and dielectric constant for both well and barrier regions versus the temperature for $In_{.1}Ga_{.9}N/GaN$ DQWs.

T (K)	**Effective mass** (m_0)		**Dielectric constant** (ε_0)		**Barrier height** (meV)
	well	**Barrier**	**barrier**	**Well**	
0	0.182	0.199	10.15	9.51	286.57
300	0.179	0.196	10.43	9.80	284.09
900	0.168	0.184	11.04	10.40	273.27

Figure 3 exhibits the variations of 1S-, 2S- and 2P-states binding energies in DRQWs, DPQWs and DTQWs according to the well width for 3 different values of the temperature. This figure indicates that with decreasing the well width, the binding energy increases reaching a maximum value around the effective Bohr radius and then decreases. The physical reason can be given as follows: A well width diminishing leads to an increment of the quantum localization of the electron wave function which reduces the mean relative electron - impurity distance. Then the binding energy can only increases. Additionally, the behavior of the 2P-state is quite different from 1S and 2S states. This result is in good agreement with those reported in [33-35]. Moreover, it can be seen that the temperature increasing induces a noteworthy drop of the binding energy for all well widths. According to **Table 2**, one can deduce that with temperature increasing the kinetic and potential barrier terms (Eq. (1)) are found to be dropped while the electro-impurity Coulomb interaction is enhanced. Our obtained results show that diminishing of the electron energy in the presence of the impurity is less than that in its absence. Our findings are in good agreement with those reported in [36].

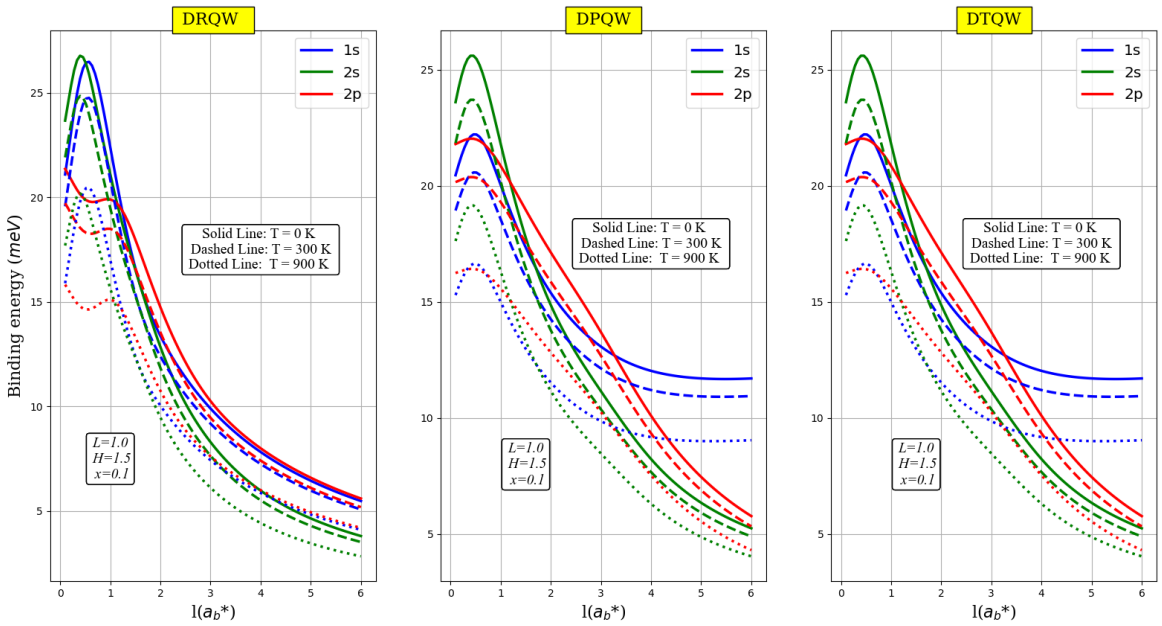

Figure 3 The 1s, 2s and 2p states-binding energy E_b as a function of the well width in a $GaN/In_{.1}Ga_{.9}N$DRQW, DPQW and DTQW for fixed parameters $L = 1$ and $H = 1.5$, for different temperature values $T = 0\ K$ (solid curve), $T = 300\ K$ (dashed curve) and $T = 900\ K$ (dotted curve).

To show more the influence of the impurity position on the binding energy, we report in **Figure 4** the variations of this latter according to the temperature for all states and all shapes. As demonstrated in **Figure 3**, the binding energy decreases as the temperature increases for a fixed impurity position. For instance, the on-center impurity binding energy difference $E_b^{1s}(0\ K) - E_b^{1s}(900\ K)$ is equal to $3.48\ meV$ for DRQWs, and $4.26\ meV$ for both DPQWs and DTQWs. Additionally, it is clearly seen that E_b is the largest for the impurity located at the structure's center while a significant drop is illustrated as this latter moves far away. This result is in good conformity with those reported in [9,10]. For instance, as the impurity is displaced from the right barrier center to the structure center, $E_b^{1s}(T = 0K)$ improvement is about 77.6 % in DRQWs whereas it exceeds 91.4 % in DPQWs and DTQWs.

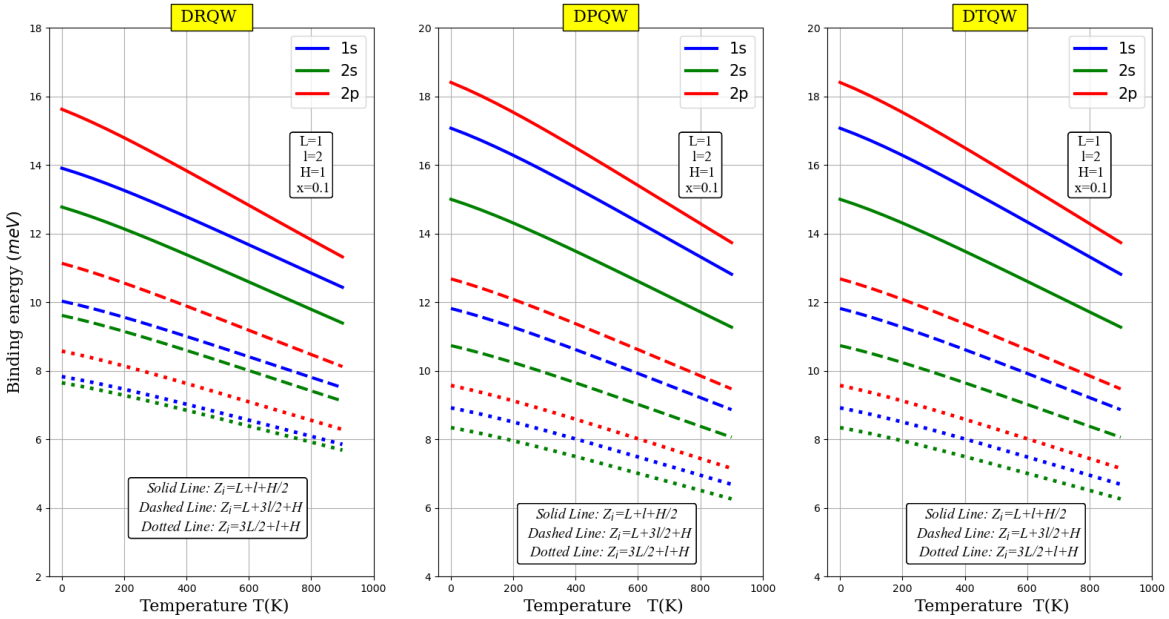

Figure 4 Variation of 1S, 2S and 2P-states binding energy with temperature in DRQWs, DPQWs and DTQWs for fixed parameters $x = 0.1, L = 1, H = 1$ and $l = 2$ with donor impurities located in the structure center (solid curve), in the right well center (dashed curve) and in the right barrier center (dotted curve).

Finally, we report in **Figure 5** the variation of binding energy of an on-center shallow donor impurity versus the side barrier width for diverse values of the coupling barrier width (H) and fixed parameters $x = 0.1$ and $T = 300\ K$. The behavior of the ground state binding energy as a function of L is similar to that found in our previous work [37] for simple and double rectangular QWs, i.e., the binding energy augments (drops) with decreasing the barrier width for a low (strong) confinement regime. The physical reason is that for strong confinement, the entire wave function is in the barrier, the more the barrier width increases the more the wave function spreads in the barrier which reduces the binding energy. In parallel, for low confinement, with increasing the barrier width the wave-function spread in the barrier diminishes which leads to enhance the binding energy. The same figure (inset) contains the variation of the 2S and 2P states binding energy versus the barrier width. It increases for reaching a maximum and then it decreases as the barrier width increases. Moreover, the binding energy drops as the coupling barrier width increases. For instance, the 1S-binding energy drop rate is about 8.5 % in DRQW and 20.8 % in both DPQW and DTQW. This result can be attributed to the lowering of the wave-functions overlapping in both wells.

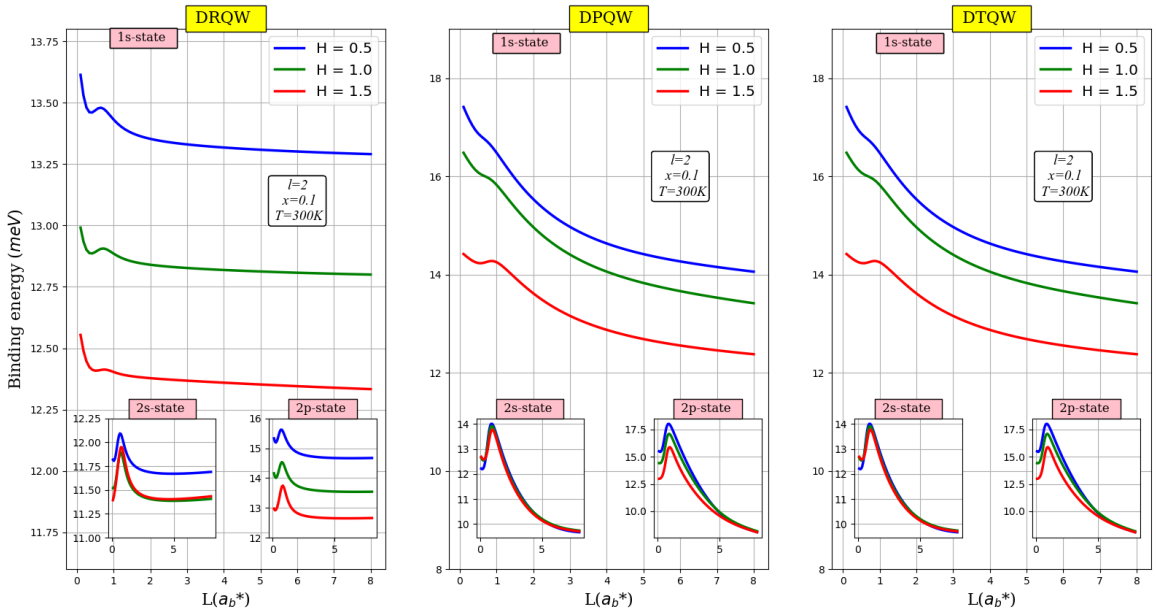

Figure 5 The ground, 2S and 2P states binding energy of an on-center hydrogenic impurity as a function of the side barrier's width of DRQWs, DPQWs and DTQWs for different coupling barrier widths $H = 0.5, 1.0$ and 1.5 with an indium content $x = 0.1, l = 2$ and $T = 300\ K$.

Conclusions

Within the effective-mass and parabolic band approximations, the 1S, 2S- and 2P-states energies with and without the impurity have been calculated in InGaN/GaN DQWs. The temperature, size and impurity's position effects are investigated for finite rectangular, parabolic and triangular confinement potential-shapes. The effective-mass, dielectric constant, band-gap energy and potential barrier temperature dependencies have been considered. Our obtained results reveal that: The binding energy is enhanced versus the coupling effect. It is reduced as a function of displacement of the impurity far away from the structure center. A significant binding energy drop is shown versus the temperature increasing. The binding energy is the highest in DPQWs and DTQWs compared to DRQWs. We believe that our study makes an important contribution to the literature. We hope that these calculation results can inspire and stimulate further researches for optoelectronic device applications related to the group of III-nitride materials.

References

[1] JY Chang, SH Yen, YA Chang and YK Kuo. Simulation of high efficiency GaN/InGaN p-i-n solar cell with suppressed polarization and barrier effects. *IEEE J. Quant. Electron*. 2013; **49**, 17-23.

[2] J Wu, W Walukiewicz, KM Yu, W Shan and JW Ager. Superior radiation resistance of $In_{1-x}Ga_xN$ alloys: Full solar-spectrum photovoltaic material system. *J. Appl. Phys.* 2013; **94**, 6477-82.

[3] JJ Wierer, AJ Fischer and DD Koleske. The impact of piezoelectric polarization and nonradiative recombination on the performance of (0001) face GaN/InGaN photovoltaic devices. *Appl. Phys. Lett*. 2010; **96**, 051107.

[4] A Mesrane, A Mahrane, F Rahmoune and A Oulebsir. Temperature dependence of InGaN dual-junction solar cell. *J. Electron. Mater*. 2017; **46**, 2451-9.

[5] H Li, W Zhao, Y Liu, Y Liang, L Ma, M Zhu, C Yi, L Xiong and Y Gao. High-level-Fe-doped P-type ZnO nanowire array/n-GaN film for ultravioletfree white light-emitting diodes. *Mater. Lett.* 2019; **239**, 45-7.

[6] MD Brubaker, KL Genter, A Roshko, PT Blanchard, BT Spann, TE Harvey and KA Bertness. UV LEDs based on p-i-n core-shell AlGaN/GaN nanowire heterostructures grown by N-polar selective area epitaxy. *Nanotechnology* 2019; **30**, 234001.

[7] I Vurgaftman and JR Meyer. Band parameters for nitrogen-containing semiconductors. *J. Appl. Phys*. 2003; **94**, 3675-96.

[8] H El Ghazi and A Jorio. Temperature dependence of interband recombination energy in symmetric (In,Ga)N spherical quantum dot-quantum well. *Phys. B Condens. Matter* 2014; **432**, 64-6.

[9] AM Elabsy. Effect of the Gamma-X crossover on the binding energies of confined donors in single GaAs/Al_xGa_{1x}As quantum-well microstructures. *J. Phys. Condens. Matter* 1994; **6**, 10025.

[10] P Nithiananthi and K Jayakumar. Diamagnetic susceptibility of hydrogenic donor impurity in low-dimensional semiconducting systems. *Solid State Comm*. 2006; **137**, 427-30.

[11] R Khordad. Effect of temperature on the binding energy of excited states in a ridge quantum wire. *Phys. E Low Dimens. Syst. Nanostruct.* 2009; **41**, 543-7.

[12] E Iqraoun, A Sali, A Rezzouk, E Feddi, F Dujardin, ME Mora-Ramos and CA Duque. Donor impurity-related photoionization cross section in GaAs cone-like quantum dots under applied electric field. *Phil. Mag*. 2017; **97**, 1445-63.

[13] L Aderras, A Bah, E Feddi, F Dujardin and CA Duque. Stark-shift of impurity fundamental state in a lens shaped quantum dot. *Phys. E Low Dimens. Syst. Nanostruct.* 2017; **89**, 119-23.

[14] H El Ghazi, R En-nadir, H Abboudi, F Jabbouti, A Jorio and I Zorkani. Two-dimensional electron gas modeling in strained InN/GaN hetero-interface under pressure and impurity effects. *Phys. B Condens. Matter* 2020; **582**, 411951.

[15] H El Ghazi, A Jorio and I Zorkani. Pressure-dependent shallow donor binding energy in InGaN/GaN square QWWs. *Phys. B Condens. Matter.* 2013; **410**, 49-52.

[16] A Sali and H Satori. The combined effect of pressure and temperature on the impurity binding energy in a cubic quantum dot using the FEM simulation. *Superlattice. Microst.* 2014; **69**, 38-52.

[17] R En-nadir, H El Ghazi, A Jorio and I Zorkani. Ground-state shallow-donor binding energy in (In,Ga)N/GaN double QWs under temperature, size and the impurity position effects. *J. Model. Simulat. Mater.* 2021; **4**, 1-6.

[18] K Batra and V Prasad. Finite difference calculation of optical properties of hydrogenic impurity in spherical quantum dot with parabolic confinement. *Revista Mexicana de Física E* 2018; **64**, 7-15.

[19] A Boda. Magnetic moment and susceptibility of an impurity in a parabolic quantum dot. *J. Magn. Magn. Mater.* 2019; **483**, 83-8.

[20] M Şahin and M Tomak. Electronic structure of a many-electron spherical quantum dot with an impurity. *Phys. Rev. B* 2005; **72**, 125323.

[21] S Wei and Q Chang. Hydrogenic impurity states in zinc-blende symmetric InGaN/GaN multiple quantum dots. *Phys. E Low Dimens. Syst. Nanostruct*. 2010; **43**, 354-8.

[22] E Sadeghi and E Naghdi. Effect of electric and magnetic fields on impurity binding energy in zinc-blend symmetric InGaN/GaN multiple quantum dots. *Nano Convergence* 2014; **1**, 25.

[23] JJ Liu, M Shen and SW Wang. The influence of compressive stress on shallow-donor impurity states in symmetric GaAs-$Ga_{1-x}Al_x$As double quantum dots. *J. Appl. Phys*. 2007; **101**, 073703.

[24] J Zheng. Binding energy of hydrogenic impurity in GaAs/$Ga_{1-x}Al_x$As multi-quantum-dot structure. *Phys. E Low Dimens. Syst. Nanostruct.* 2008; **40**, 2879-83.

[25] CP Liu, YL Lai and ZQ Chen. Interface characterization and indium content of indium-rich quantum dots in InGaN/GaN multiple quantum wells. *Appl. Surf. Sci.* 2006; **252**, 3922-7.

[26] E Kasapoglu. Binding energy of donor impurities in double inverse parabolic quantum wells under electric field. *Phys. E Low Dimens. Syst. Nanostruct.* 2009; **41**, 1222-5.

[27] H Akbas, C Dane, I Erdogan and O Akankan. Hydrogenic donor in asymmetric $Al_{xL}Ga_{1-xL}$As/GaAs/$Al_{xR}Ga_{1-xR}$As quantum wells. *Phys. E Low Dimens. Syst. Nanostruct.* 2014; **60**, 196-9.

[28] J Zhu, SL Ban and SH Ha. Built-in electric field effect on donor impurities in strained Wurtzite GaN/AlGaN asymmetric double quantum wells. *Mod. Phys. Lett. B* 2012; **26**, 1250172.

[29] YP Varshni. Temperature dependence of the energy gap in semiconductors. *Physica* 1967; **34**, 149-54.

[30] H El Ghazi, A Jorio and I Zorkani. Pressure-dependent of linear and nonlinear optical properties of (In,Ga)N/GaN spherical QD. *Superlattic. Microst*. 2014; **71**, 211-6.

[31] MH Gazzah, B Chouchen, A Fargi and H Belmabrouk. Electro-thermal modeling for $In_xGa_{1-x}N$/GaN based quantum well heterostructures. *Mater. Sci. Semicond. Process*. 2019; **93**, 231-7.
[32] W Belaid, H El Ghazi, I Zorkani and A Jorio. Pressure-related binding energy in (In,Ga)N/GaN double quantum wells under internal composition effects. *Solid State Comm.* 2021; **327**, 114193.
[33] M Barati, G Rezaei and MRK Vahdani. Binding energy of a hydrogenic donor impurity in an ellipsoidal finite-potential quantum dot. *Phys. Status Solidi* 2007; **244**, 2605-10.
[34] RD Bella and K Navaneethakrishnan. Donor binding energies and spin - orbit coupling in a spherical quantum dot. *Solid State Comm*. 2004; **130**, 773-6.
[35] G Rezaei, N Doostimotlagh and B Vaseghi. Simultaneous effects of hydrostatic pressure and conduction band non-parabolicity on binding energies and diamagnetic susceptibility of a hydrogenic impurity in spherical quantum dots. *Comm. Theor. Phys*. 2011; **56**, 377.
[36] E Kasapoglu. The hydrostatic pressure and temperature effects on donor impurities in GaAs/$Ga_{1-x}Al_xAs$ double quantum well under the external fields. *Phys. Lett. A* 2008; **373**, 140-3.
[37] W Belaid, H El Ghazi, I Zorkani and A Jorio. Impact of QW coupling on the binding energy in InGaN/GaN under the effects of the size, the impurity and the internal composition. *MATEC Web Conf*. 2020; **330**, 01012.